

TECHNICAL REPORT

Landscape and Watershed Processes

Watershed-scale spatial prediction of agricultural land phosphorus mass balance and soil phosphorus metrics: A bottom-up approach

Finn A. Bondeson¹ | Joshua W. Faulkner^{1,2,3} | Tiffany L. Chin⁴ |
Andrew W. Schroth^{4,5}  | Michael Winchell⁶ | Aubert Michaud⁷ | Mohamed Niang⁸ |
Eric D. Roy^{1,3,4} 

¹Department of Civil and Environmental Engineering, University of Vermont, Burlington, Vermont, USA

²Department of Plant and Soil Science, University of Vermont, Burlington, Vermont, USA

³Gund Institute for Environment, University of Vermont, Burlington, Vermont, USA

⁴Rubenstein School of Environment and Natural Resources, University of Vermont, Burlington, Vermont, USA

⁵Department of Geography and Geosciences, University of Vermont, Burlington, Vermont, USA

⁶Stone Environmental, Montpelier, Vermont, USA

⁷Organisme de bassin versant de la baie Missisquoi, Bedford, Quebec, Canada

⁸Institut de recherche et de developpement en agroenvironnement, Québec, Quebec, Canada

Correspondence

Eric D. Roy, Rubenstein School of Environment and Natural Resources, University of Vermont, Burlington, VT, USA. Email: eroy4@uvm.edu

Assigned to Associate Editor Heidi Peterson.

Funding information

National Oceanic and Atmospheric Administration, Grant/Award Number: NA22NWS4320003; Lake Champlain Basin Program, Grant/Award Number: LC00A00707

Abstract

Analysis of nutrient balance at the watershed scale, including for phosphorus (P), is typically accomplished using aggregate input datasets, resulting in an inability to capture the variability of P status across the study region. This study presents a set of methods to predict and visualize partial P mass balance, soil P saturation ratio (PSR), and soil test P for agricultural parcels across a watershed in the Lake Champlain Basin (Vermont, USA) using granular, field-level data. K-means cluster analyses were used to group agricultural parcels by soil texture, average slope, and crop type. Using a set of parcels accounting for ~21% of the watershed's agricultural land and having known soil test and nutrient management parameters, predictions of partial P mass balance, PSR, and soil test P for agricultural land across the watershed were made by cluster, incorporating uncertainty. This resulted in an average partial P balance of 5.5 ± 0.2 kg P ha⁻¹ year⁻¹ and an average PSR of 0.0399 ± 0.0002 . Furthermore, approximately 30% of agricultural land had predicted soil test P values above optimum levels. Results were used to visualize areas with high P loss potential. Such data

Abbreviations: CLU, common land unit; CSA, critical source area; GIS, ArcGIS Pro; LFO, large farm operation; M3, Mehlich-3; MBB, Vermont portion of the Missisquoi Bay Basin; MM, Modified Morgan; NHDPlus HR, National Hydrography Dataset Plus High Resolution; NMP, nutrient management plan; PSR, phosphorus saturation ratio; USEPA, United States Environmental Protection Agency; USGS, United States Geological Survey; VAAFM, Vermont Agency of Agriculture, Food, and Markets; VCGI, Vermont Center for Geographic Information.

This is an open access article under the terms of the [Creative Commons Attribution-NonCommercial-NoDerivs](https://creativecommons.org/licenses/by-nc-nd/4.0/) License, which permits use and distribution in any medium, provided the original work is properly cited, the use is non-commercial and no modifications or adaptations are made.

© 2024 The Author(s). *Journal of Environmental Quality* published by Wiley Periodicals LLC on behalf of American Society of Agronomy, Crop Science Society of America, and Soil Science Society of America.

and visualizations can inform watershed P modeling and assist practitioners in nutrient management decision making. These techniques can also serve as a framework for bottom-up modeling of nutrient mass balance and soil metrics in other regions.

Plain Language Summary

Excessive inputs of phosphorus (P) to aquatic ecosystems can result in undesirable effects, including harmful algal blooms. Efforts are underway to improve management of P, an essential nutrient for plant growth, in watersheds across the United States and elsewhere. As part of these efforts, it is important to assess soil P levels and P mass balance (inputs to soils minus outputs from soils). Here, we present methods to predict and visualize soil P metrics and partial P mass balance for agricultural parcels across a watershed using field-level data. Our study is based in a watershed within the Lake Champlain Basin (Vermont, USA). We predict an average partial P balance of $5.5 \text{ kg P ha}^{-1} \text{ year}^{-1}$ for agricultural land, with 30% of agricultural land area characterized by soil test P values greater than optimum levels. We visualize these results using maps and discuss how these techniques can be useful in other regions.

1 | INTRODUCTION

Excess phosphorus (P) loading to surface waters contributes to eutrophication, symptoms of which can include harmful algal blooms, oxygen depletion, and fish kills (Correll, 1998). Watershed-scale P mass balance analyses are integral to assessing P flows and informing water quality initiatives, and various impaired watersheds have been analyzed in recent years (Engel et al., 2013; Jaworski et al., 1992; Maccoux et al., 2016; Meals et al., 2008a; Roy et al., 2014; Scavia et al., 2019). Such analyses are particularly important in agricultural areas, as it is well documented that nonpoint source losses from agricultural land account for a substantial portion of terrestrial P export in such watersheds (Engel et al., 2013; Maccoux et al., 2016; Scavia et al., 2019). In step with watershed-scale mass balance analysis, numerous efforts have been made to identify P critical source areas (CSAs) within a landscape (i.e., areas that are at highest risk of contributing to nonpoint source P pollution) (e.g., Heathwaite et al., 2003), including in the Lake Champlain Basin (Michaud et al., 2007; Meals et al., 2008b; Ghebremichael et al., 2010; Winchell et al., 2011).

The computational ability to model P movement has increased considerably in recent decades, prompting an increase in nutrient mass balance and transport modeling globally (Z. Wang et al., 2020). However, issues have arisen in scaling between models of various sizes, including data overgeneralization, overparameterization, uncertainty, and high computational demand (Radcliffe et al., 2009; Z. Wang et al., 2020). Past studies have typically relied on aggregated county,

state, regional, or federal data sources and used these data to make broad assumptions across the landscape. For example, Meals et al. (2008b) consulted with industry and government experts to establish a single manure application rate and soil test P value for each crop type, and Winchell et al. (2011) derived animal populations and subsequent manure application rates from 2007 USDA Census of Agriculture data for each county/subwatershed/crop type combination. Such approaches based on aggregated data are common within the broader literature (Chowdhury et al., 2014).

Although many watershed-scale analyses make good use of aggregated data, they also make broad assumptions about data generalizability. While aggregated data may accurately represent a general average nutrient status within a region, variability in P flows and soil metrics occurring across the region and uncertainty are not well accounted for. This homogeneity of data across a watershed limits the ability of a model to represent conditions at smaller spatial scales within the watershed, which inherently obscures high-risk areas that can play important roles in P loading to surface waters (i.e., CSAs).

To our knowledge, no analyses or methods have been conducted that apply granular field-scale data, such as that used for farm-level nutrient mass balances, to make spatially heterogeneous mass balance and nutrient status predictions at the watershed scale. Given the current gap between farm scale and regional or watershed-scale P data use, management, and decision making, we developed methods in this study that use field-level data from farm nutrient management plans (NMPs)

to predict partial P mass balance and key soil test parameters for all agricultural land in the Vermont portion of the 184,297-ha Missisquoi Bay Basin (MBB). The results from the model described in this work will inform a comprehensive binational modeling project (Supporting Information S1). Our work can also inform watershed-scale nutrient mass balance research in other locations.

2 | MATERIALS AND METHODS

2.1 | Study region

The Missisquoi Bay watershed spans the border of the United States and Canada in Vermont and Quebec, and drains to Missisquoi Bay, a shallow bay connected to the larger Lake Champlain. Due to high historic and ongoing nutrient loads, as well as consequent frequent and severe cyanobacteria blooms (LCBP, 2022), Lake Champlain is subject to USEPA total maximum daily load limits for P (USEPA, 2016). Of all of the subwatersheds within the Lake Champlain Basin, the Missisquoi Bay watershed is identified by the USEPA as presenting the “greatest challenge in attaining water quality standards” due to high nonpoint source P export (USEPA, 2016). It has been estimated that 64% of the Missisquoi Bay watershed’s total P load to Missisquoi Bay can be attributed to agricultural activity (Winchell et al., 2011). The Vermont (VT) and Quebec portions of the Lake Champlain drainage area both host considerable agricultural activity characterized by dairy farming and associated feed production. As this work focuses on only the VT portion of the binational Missisquoi Bay watershed, the abbreviation MBB will herein be used to indicate only the VT portion of the watershed.

2.2 | Model framework

The general approach of our spatial P prediction model consisted of the workflow shown in Figure 1.

2.3 | Spatial data

Spatial data analyzed in this work were processed with ArcGIS Pro (GIS) software, version 3.0.3 (Esri, 2022) and associated out-of-the-box functions and tools. The MBB boundary was defined using data from the United States Geological Survey (USGS) National Hydrography Dataset Plus High Resolution (NHDPlus HR) (Moore et al., 2019; USGS, 2022) and the Vermont Center for Geographic Information’s (VCGI) Open Geodata Portal (VCGI, 2016). Agricultural land comprised approximately 21% of the MBB watershed. An agricultural land cover layer for the MBB was developed from

Core Ideas

- Watershed-scale nutrient status predictions are typically made using aggregated datasets.
- Watershed-scale nutrient status predictions can be informed by field-level data.
- Spatial heterogeneity is preserved when using field-level data to predict nutrient status at the watershed scale.
- Granular predictions can inform regional nutrient management policy.

the VCGI Open Geodata Portal (VCGI, 2016), the USDA Cropland Data Layer (USDA NASS, 2016), and common land unit (CLU) polygons from the 2011 CSA analysis of the MBB (Winchell et al., 2011). Notably, the CLU polygons were used to define field boundaries, increasing the layer’s ability to represent spatial variability in soils and nutrient management data. See Supporting Information S2 for additional details. Based on data sources, polygons were assigned typologies of corn, hay, pasture, soybean, and “other agricultural”. A total of 5557 fields were established, totaling 35,688 ha. Typology percentages by agricultural land area were 75% hay and other forages, 23% corn, 1.2% pasture, and <1% soybean and other agricultural.

2.4 | Nutrient management plans

As input data for P analysis, 10 NMPs prepared for the 2022 growing season from dairy farms operating within the MBB were provided by the Vermont Agency of Agriculture, Food, and Markets (VAAFAM). All 10 farms were categorized as large farm operations (LFOs) by the VAAFAM (>700 mature dairy cows). NMPs provided acreage, cropping, nutrient management, and soil test information for each individual field unit managed by the 10 producers, as well as GIS polygon data for each field, to which we attributed that field’s data. We have considered this group representative due to the dominance of dairy farming in the region (USDA NASS, 2017).

The NMPs contained a total of 7347 ha of agricultural land, accounting for approximately 21% of the total agricultural land area in the MBB. The total area managed by each farm in our 10-farm dataset ranged from 145 to 2096 ha, capturing the variability of farm size within the region. There were 1422 fields included in the dataset, with sizes ranging from 0.08 to 49.9 ha. Hay accounted for 4363 ha, or 59.4% and corn accounted for 2984 ha, or 40.6%, of the agricultural land in the NMPs. In relation to the MBB, the NMPs accounted for 16.2% of hay and 38.2% of corn cropping basin wide. When visually

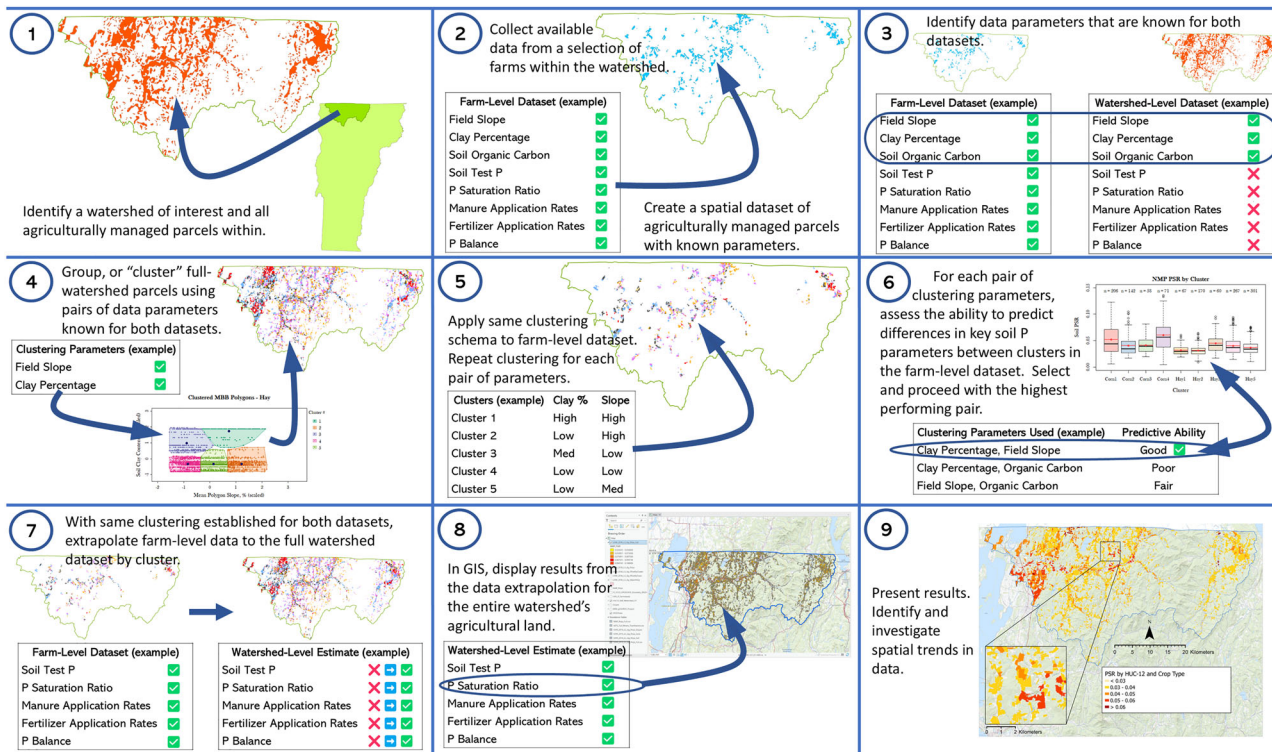


FIGURE 1 Steps to extrapolate farm-level nutrient management and soil test data to agricultural land at the watershed scale.

inspected in GIS, the set of NMP polygons followed similar spatial distribution to agricultural land across the MBB. This spatial alignment increased the applicability of the NMPs to the entire watershed’s agricultural land.

However, we recognize that the NMP polygon dataset from a limited number of LFOs may bias the dataset. For example, of the 7347 ha of agricultural land included in the NMPs, 0 ha were categorized as either pasture, soybean, or other agriculture, which together accounted for <2% of the watershed agricultural land area. Assumptions made for assigning nutrient management and soil test data to these land use types are addressed in Supporting Information S3. Also, the LFOs included in this work are by nature larger and more livestock-intensive than farms not required to compile NMPs (Hall & Essman, 2019). That said, manure is the dominant P source to agricultural land in the watershed (approximately eight times more manure P than fertilizer P; Sabo et al., 2021), and the NMP dataset retains high value in its granular nature and spatial specificity compared to aggregate data (e.g., county-level), which is also subject to uncertainty. We account for uncertainty in our estimate of MBB partial P mass balance and spatial extrapolation (see Section 2.6.4).

2.5 | Soils and topography

For each polygon in the MBB and NMP datasets, we compiled data on soil clay percentage, soil organic carbon percent-

age, and soil pH from the Soil Survey Geographic database (NRCS, 2022), and mean parcel slope from the USGS’s NHD-Plus HR (Moore et al., 2019; USGS, 2022). See Supporting Information S4 and S5 and Table S1 for more details.

2.6 | Data analysis

We performed data manipulation, calculation, plotting, and statistical analysis using R software (R Core Team, 2022) (see Supporting Information S6). Statistical inferences were conducted using Kruskal–Wallis non-parametric tests with multiple post hoc Dunn–Bonferroni pairwise comparisons to assess differences between grouped data. We identified $p < 0.05$ as the threshold for significant results.

2.6.1 | K-means cluster analysis

To find similarities between the NMP and MBB datasets, we employed K-means clustering (Hartigan & Wong, 1979). After clustering the MBB agricultural land and finding the centroids of each cluster, we clustered the NMP data around those centroids. We were then able to extrapolate nutrient management and P, AI, and phosphorus saturation ratio (PSR) data from NMPs in each cluster to the MBB fields in that same cluster. Note that clustering was done separately for the two dominant crop types: corn and hay. Methods to determine the

best clustering parameters (slope and soil clay content) and number of clusters are given in Supporting Information S6 and S7 and Figure S1.

2.6.2 | Estimating agricultural land partial P mass balance

During extrapolation, we applied the per-cluster mean values of manure application rates, fertilizer application rates, and crop uptake P rates from the NMP clusters to the MBB clusters. Detailed methods used to proportionally allocate manure, fertilizer, and crop uptake information from the NMPs to the MBB dataset are given in Supporting Information S8. After extrapolation, we calculated a partial P mass balance ($\text{kg P ha}^{-1} \text{ year}^{-1}$) for each agricultural land parcel as P applied via manure plus P applied via fertilizer minus crop P uptake. This partial mass balance does not account for P losses to water.

Note that we assumed a value of “0” for nutrient mass balance for agricultural land categorized as pasture, other ag, or soybean due to their combined contribution of <2% of agricultural land, and to be in agreement with pasture grazing/dung dropping balance assumptions made by Meals et al. (2008b). We also did not account for atmospheric deposition into nor leaching/export via surface waters out of the system boundary (hence, the “partial” mass balance). To achieve this partial P mass balance for the entire watershed, we multiplied the result of each per-field mass balance rate by the area of that field (in ha) to produce a net P excess or deficit for each field. We then summed these to find a net partial mass balance for the MBB.

2.6.3 | Estimating soil P saturation (PSR) and soil test P

Unlike manure and fertilizer application rates only applicable to some fields in the NMPs for some time periods, we had values of Modified Morgan P (MMP) and Modified Morgan Al (MMAI) directly from NMPs, as well as Mehlich-3 P (M3P), Mehlich-3 Al (M3AI), and P saturation ratio (calculated) for all fields. After clustering the NMP dataset, each cluster had a unique distribution of values for these soil test parameters. To preserve variability of the NMP clusters in MBB predictions, we assigned the same distribution of PSR values from each cluster in the NMP dataset to its corresponding cluster in the MBB dataset. For each PSR observation pulled, we pulled along the associated MMP, MMAI, M3P, and M3AI.

2.6.4 | Data extrapolation, uncertainty, and visualization

There are a few limitations to the methods described thus far. First, applying the in-cluster means of nutrient balance param-

eters discards some of the variability present in the NMPs. Second, when assigning a proportion of MBB fields in each cluster with manure or fertilizer application values, we chose those fields randomly. This means that each iteration of this redistribution is only one of numerous possible outcomes.

To counteract the possibility that random chance would produce results far away from the theoretical “mean” situation, we ran the NMP → MBB extrapolation 10,000 times. For each of the 10,000 unique iterations, we calculated and saved the mean value of the following parameters of the MBB dataset: per-ha P balance, corn cropland per-ha P balance, hay cropland per-ha P balance, PSR, corn cropland PSR, and hay cropland PSR. For each iteration, we also saved the value of net partial P balance and calculated the total proportion (by area) of the MBB that received a PSR observation of >0.1, the broadly applicable M3-PSR threshold value identified by Dari et al. (2018). This approach resulted in distributions of possible results for each parameter, helping to clarify uncertainty.

Lastly, we repeated iterations of the NMP → MBB extrapolation model until it produced an output with means < $10.1 \times \text{SDI}$ away from the mean values of 10,000 runs for per-ha P balance and PSR, and < $10.25 \times \text{SDI}$ away from the mean values of 10,000 runs for corn cropland per-ha P balance, hay cropland per-ha P balance, corn cropland PSR, and hay cropland PSR. We refer to this result as the “centrally trending model iteration” and regard this model iteration as being as close to the theoretical mean basin-wide extrapolation as practical.

To protect farmer privacy when displaying the prediction in GIS, we performed some minor aggregation. We computed spatially weighted mean values of P balance, PSR, and MMP for the centrally trending model iteration within each combination of land use type and NHDPlus HR HUC-12 subwatershed. A total of 25 HUC-12-level subwatersheds existed in the MBB, with 82 distinct combinations of HUC-12 and land use type. Spatially weighted means were computed by multiplying each field’s P balance rate by the field’s area, summing these totals within one HUC-12/land use type group, then dividing by the total area of all fields in that group. This provided smoother visualization of trends by cluster across the landscape, highlighting areas with higher or lower P parameter values, as opposed to individual fields. Second, smoothing the data for public representation reinforces that the model is an informed estimate of spatial P saturation and soil test P conditions for agricultural land types across the MBB but should not be used to make field-level conclusions.

3 | RESULTS

3.1 | K-means clustering

Cluster agreement between the two datasets (NMP and MBB) was comparable, and the MBB → NMP cluster assignment

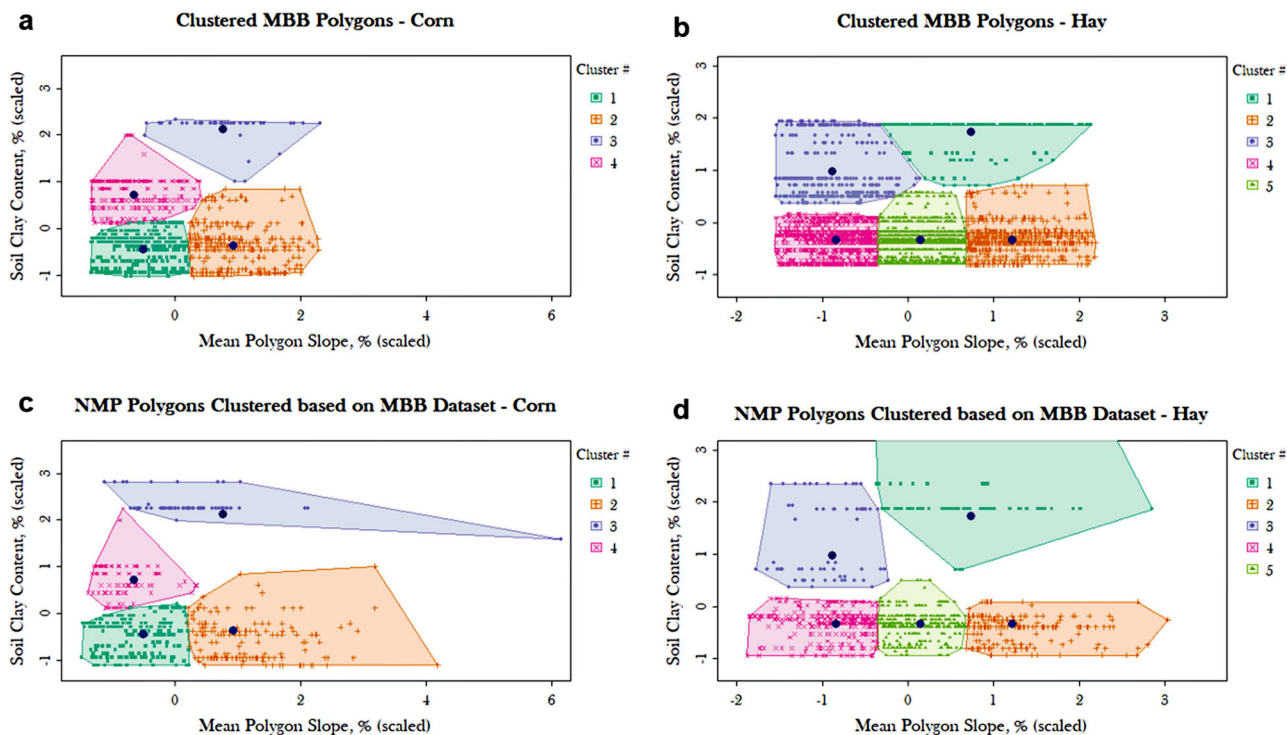


FIGURE 2 Clustered agricultural land for the Vermont Missisquoi Bay Basin (MBB) (a and b) and the nutrient management plan (NMP) data (c and d). Due to a small number of outlying observations of 100% clay percentage in hay cluster 1, Plot 2d was truncated to better display clusters 2, 3, 4, and 5.

was considered successful (Figure 2). Note that the range of the NMP data is higher, as outliers were not trimmed from this dataset when clustering. Pairwise statistical comparison revealed that 100% of the cluster comparisons were statistically different by either slope, clay, or both. See Figure S2 and Table S2 for further details.

3.2 | Agricultural land partial P mass balance

After clustering was applied to the NMP dataset, 15 of the 36 possible pairwise comparisons between P balance of the clusters, or 42%, were statistically different from each other. Once applied to the MBB in the centrally trending iteration, the distributions remained markedly similar. We observed strong central tendencies after the 10,000 runs for each cluster's mean partial P balance, where we observed significant differences for 35 of the 36 possible comparisons, or 97%, between clusters in the MBB (see Figure S3).

Furthermore, we calculated the net partial P balance for the MBB for each of the 10,000 model runs, and a normal distribution was achieved (see Figure S4). The mean agricultural land partial P balance for the MBB watershed was $196,249 \pm 7861$ kg P year⁻¹ ($449,411 \pm 18,001$ kg P₂O₅ year⁻¹). The distributions of per hectare partial P balance for the watershed, and for corn and hay cropland separately, were

similarly normal over the 10,000 iterations. The MBB had an average P balance of 5.5 ± 0.2 kg P ha⁻¹ year⁻¹ (12.6 ± 0.5 kg P₂O₅ ha⁻¹ year⁻¹) for all agricultural land, 13.3 ± 0.8 kg P ha⁻¹ year⁻¹ (30.5 ± 1.8 kg P₂O₅ ha⁻¹ year⁻¹) for corn cropland, and 3.2 ± 0.2 kg P ha⁻¹ year⁻¹ (7.4 ± 0.4 kg P₂O₅ ha⁻¹ year⁻¹) for hay. Figure 3 shows partial P balance predictions for the MBB agricultural land for the centrally trending model iteration, aggregated by subwatershed and land use type.

3.3 | Phosphorus saturation ratio (PSR)

After clustering was applied to the NMP dataset, 20 of the 36 possible pairwise comparisons between PSR of the clusters were statistically different from each other. Once applied to the MBB in the centrally trending model iteration, the distributions remained markedly similar. We observed strong central tendencies after the 10,000 runs for each cluster's mean PSR, where we observed significant differences for 32 of the 36 possible comparisons between clusters in the MBB (see Figure S5).

As with P balance, a normal distribution for mean PSR of MBB agricultural land was achieved when the model was run 10,000 times (Figure S6). We found that the average agricultural parcel in the MBB had a PSR of 0.0399 ± 0.0002 , while corn and hay cropland (both also showing normal

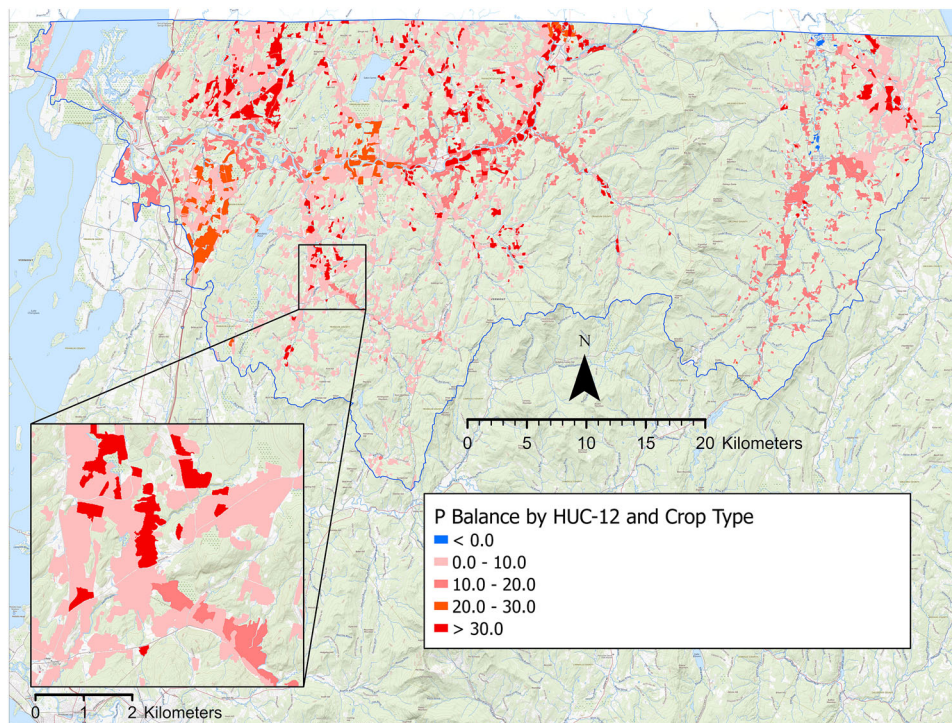


FIGURE 3 Partial P balance predictions ($\text{kg P ha}^{-1} \text{ yr}^{-1}$) for Missisquoi Bay Basin (MBB) agricultural land displayed by HUC-12 and crop type for one centrally trending model iteration. These results are spatial estimates and should not be interpreted as actual P balance values of real fields. The blue outline is the MBB watershed boundary (Vermont portion only).

distributions) had PSR means of 0.0492 ± 0.0008 and 0.0373 ± 0.0002 , respectively.

We also evaluated the P loss potential predicted by the model. In keeping with the PSR threshold of 0.1 proposed by Dari et al. (2018), we calculated the percentage of the watershed's area with a PSR > 0.1 for each of the 10,000 runs. For each iteration of the model, some number of fields was allocated a PSR > 0.1 and the acreage of these fields was summed. Over the 10,000 runs, the mean percentage of the MBB agricultural land at highest risk for P loss was $1.7\% \pm 0.2\%$. Note that all fields receiving a PSR > 0.1 in the NMP \rightarrow MBB extrapolation were corn fields. Figure 4 shows PSR predictions for the MBB agricultural land for the centrally trending model iteration, aggregated by subwatershed and land use type.

3.4 | Modified Morgan P (MMP)

In the centrally trending model iteration (Figure 5), approximately 6% of the MBB's agricultural land had "low" MMP concentrations, 25% was "medium," 38% was "optimum," 29% was "high," and 2% was "excessive," based on MMP interpretation recommendations developed by the University of Vermont Extension (Jokela et al., 2020). Excessive MMP was therefore similar in prevalence to PSR values > 0.1 .

3.5 | By-cluster results

Key results of our clustering and data analysis are shown in Table 1, with PSR and P balance ranked by cluster. The corn cluster with medium slope and high soil clay content had the highest P balance ($27 \pm 1 \text{ kg P ha}^{-1} \text{ year}^{-1}$), other corn clusters had mean P balances ranging from 6 to 19 $\text{kg P ha}^{-1} \text{ year}^{-1}$, and all hay clusters had mean P balances between 1 and 8 $\text{kg P ha}^{-1} \text{ year}^{-1}$. Cluster-mean PSR and P balance values were not correlated (Spearman rho = 0.36; $p = 0.34$).

4 | DISCUSSION

4.1 | Agricultural land partial P mass balance

As stated in Section 2.4, our use of a limited number of NMPs inherently carries risk of bias, particularly due to inclusion of only LFOs that engage in dairy farming. A prior study using "top-down" methods based on county-level data for 2012 estimated total manure P and farm fertilizer P in the MBB to be 952 and 122 metric tons P, respectively (Sabo et al., 2021). Based on those basin-scale estimates, the NMPs used here accounted for approximately 33% of manure P and 9% of fertilizer P. Given that the NMPs accounted for 21%

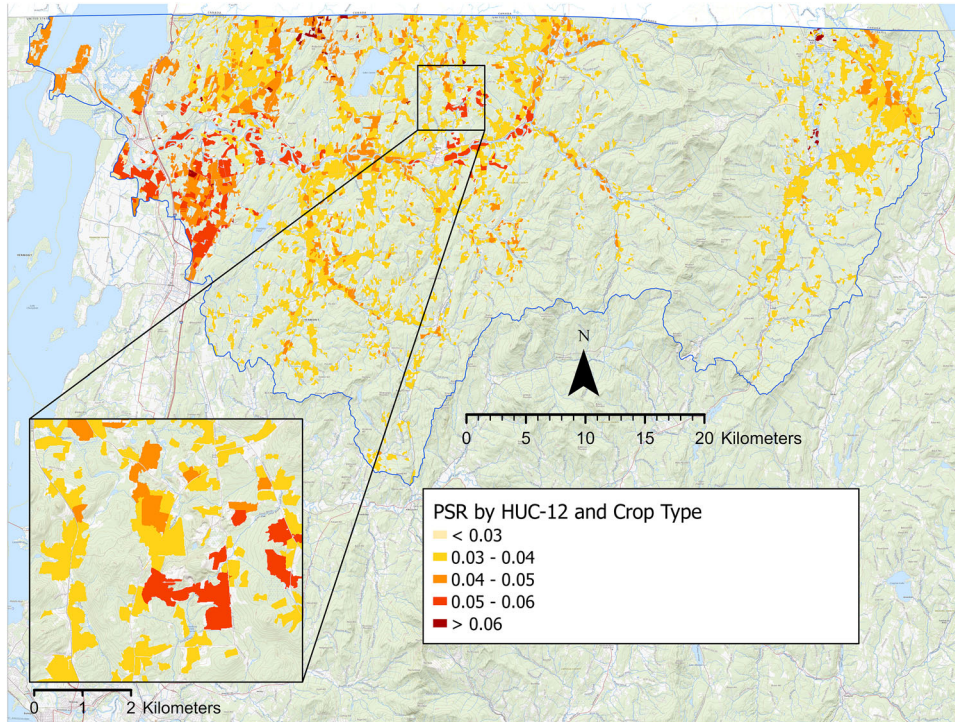


FIGURE 4 Phosphorus saturation ratio (PSR) predictions for Missisquoi Bay Basin (MBB) agricultural land displayed by HUC-12 and crop type for one centrally trending model iteration. These results are spatial estimates and should not be interpreted as actual PSR values of real fields. Note that although some individual field values were >0.1, all HUC-12/crop means were <0.1. The blue outline is the MBB watershed boundary (Vermont portion only).

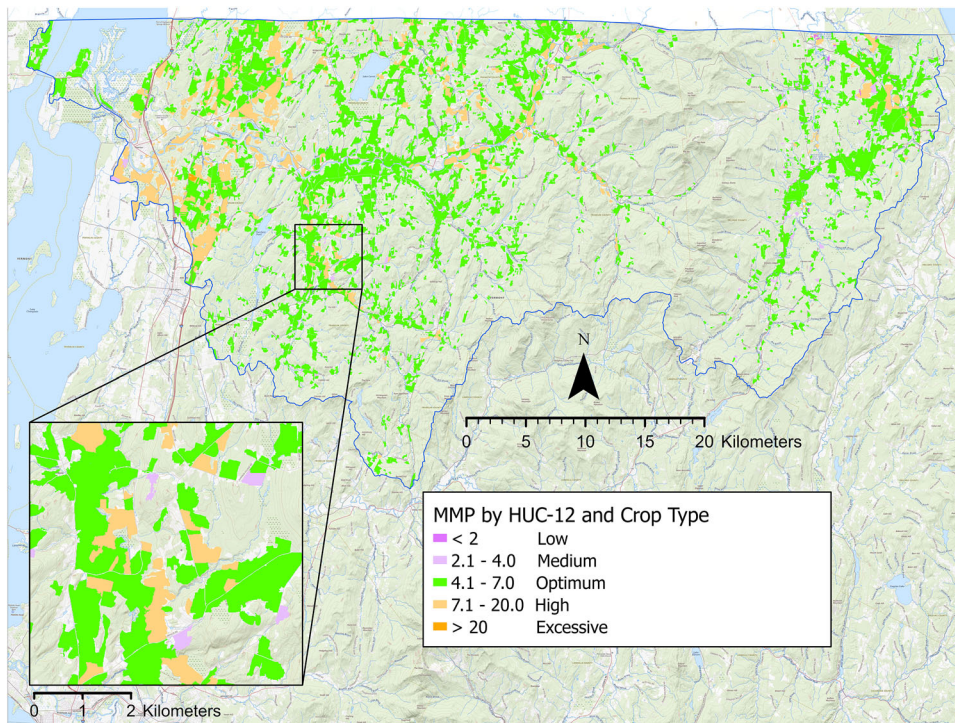


FIGURE 5 Modified Morgan P (MMP) (mg P kg^{-1}) predictions for Missisquoi Bay Basin (MBB) agricultural land displayed by HUC-12 and crop type for one centrally trending model iteration. These results are spatial estimates and should not be interpreted as actual MMP values of real fields. The blue outline is the MBB watershed boundary (Vermont portion only).

TABLE 1 By-cluster summary of 10,000 iteration results for clustered Missisquoi Bay Basin (MBB) agricultural land. Rankings having the highest phosphorus saturation ratio (PSR) or P balance are ranked with a 1. n = number of fields.

Cluster	Relative slope	Relative clay %	MBB PSR mean	PSR rank	MBB P balance mean (kg P ha ⁻¹ year ⁻¹)	P balance rank	Cluster area (ha)	Cluster area (%)	n
Corn 4	Low	Mid	0.061 ± 0.0003	1	5.65 ± 1.04	5	1737	5	213
Corn 1	Low	Low	0.052 ± 0.0002	2	10.45 ± 1.09	3	3526	10	447
Hay 3	Low	Mid	0.045 ± 0.0002	3	2.46 ± 0.48	7	3460	10	500
Corn 3	Mid	High	0.041 ± 0.0001	4	27.38 ± 1.22	1	714	2	85
Corn 2	High	Low	0.040 ± 0.0002	5	19.14 ± 1.12	2	2282	6	360
Hay 4	Low	Low	0.040 ± 0.0002	6	2.65 ± 0.48	6	7605	21	1179
Hay 5	Mid	Low	0.037 ± 0.0001	7	2.05 ± 0.48	8	9197	26	1475
Hay 1	Mid	High	0.032 ± 0.0001	8	0.93 ± 0.53	9	1859	5	287
Hay 2	High	Low	0.032 ± 0.0001	9	7.99 ± 0.52	4	4653	13	852
Others	n/a	n/a	0.045 ± 0.017	n/a	n/a	n/a	655	2	159
MBB watershed			0.0399 ± 0.0002	n/a	5.50 ± 0.22	n/a	35688	100	5557

of agricultural land, it seems that the NMP dataset may over-represent manure and underrepresent fertilizer inputs. Given our methods, it is not possible to gauge the effect of the NMP dataset being potentially biased toward fields where manure is applied. For example, fields outside the NMP dataset may use less manure and more fertilizer but maintain a similar P balance. Despite this limitation, we think our approach remains robust because manure is the dominant source of P inputs to MBB croplands (~8:1 manure:fertilizer on P basis; Sabo et al., 2021), and our efforts to account for uncertainty help clarify the potential effects of bias.

When comparing partial P balance between clusters in the NMP dataset, all statistically different comparisons were between either two corn groups or between a corn group and a hay group. Although statistical significance between groups was generally low, there is evidence that crop type, as well as slope and soil clay content characteristics, are related to P balance trends. Slope and clay appeared more influential for corn cropland due to stronger statistical differences in P balance between corn clusters. From the results of 10,000 NMP → MBB predictions, partial P balance was highest for corn cropland, consistent with previous watershed-scale P status analysis (Meals et al., 2008b). Indeed, the cluster with highest P balance values was land farmed in corn with high clay percentage on medium slopes, and the three clusters with highest P balance were all corn clusters. The cluster with the lowest P balance was hay farmed on high clay and medium slopes (Table 1).

Even after aggregating by subwatershed and land use type, spatial differences in partial P balance between different portions of the watershed were evident (Figure 3). Examination of P balance predictions across the MBB indicated that its agricultural land is operating at a P surplus, and areas with highest P surplus are located close to river corridors and in the western third of the watershed, closest to Lake Champlain. Agricultural land management and land use in the MBB watershed has historically been constrained by geography, and our analyses suggest high nutrient input to areas that are hydrologically connected to the Missisquoi River and Lake Champlain. This is especially concerning during storm events, when inundation and erosion accelerate P mobilization to the Bay through P release and sediment transport (LCBP, 2022; USEPA, 2016). Our values for agricultural land partial P mass balance are in line with or lower than most values presented in prior studies (see Table S3 and Supporting Information S9).

4.2 | PSR and MMP

Our results show that crop type, as well as soil texture and field topography, have influence on P saturation trends. The 10,000 prediction iterations illustrated that with repeated modeling,

the tendency of the NMP → MBB extrapolation was to centralize around the mean PSR of each of the clusters in the NMPs. While repeated iterations of the model forced a result toward central tendencies (i.e., made aggregate data out of granular data), it is important to note that some variability of the original NMP data was upheld through the existence of the clusters themselves. Instead of applying one mean PSR or a mean P balance rate to all agricultural land in the MBB, we demonstrated through statistical testing that PSR and P balance are to some degree linked to crop type, slope, and soil texture.

Spatial trends highlighting the more at-risk areas were evident for the MBB. The highest values for predicted PSR and MMP were concentrated around the Missisquoi River and its larger tributaries, as well as in the agricultural land west of a ridge running SSW-NNE and approximately 15 km east of the Lake Champlain shore. Overall, most of the basin is operating at “optimal” MMP levels, with the same regions high in PSR exhibiting “high” or “excessive” MMP levels (Figures 4 and 5).

Similarities between PSR and MMP were, namely, due to MMP being an input to PSR calculation. In addition to MMP soil test values being used to proxy plant availability of P (Jokela et al., 2020), they can be used alongside PSR to predict the likelihood of P loss. Greater plant-available P is associated with greater water soluble P forms in soils and subsequent risk of mobilization (Heathwaite et al., 2015; Jokela et al., 1998; Magdoff et al., 1999). It has been shown that above a certain PSR, P becomes increasingly likely to be released from soils to water in soluble form, and thus available for transport through runoff and groundwater. This PSR “change point” or “threshold” varies between soils but is consistently within the range of 0.1–0.23 (Dari et al., 2018; Khiari et al., 2000; Sims et al., 2002; Wiegman et al., 2022), depending on the soil extraction method (e.g., M3 or oxalate).

Our results for PSR and MMP basin-wide were generally lower than expected, given ongoing challenges meeting P load reductions. We regard the 1.7% of MBB agricultural land area predicted as the highest risk due to $PSR > 0.1$ as a low proportion, especially considering the higher P saturations of some soils analyzed in studies by Dari et al. (2018), Sims et al. (2002), Khiari et al. (2000), Y. Wang et al. (2015), and Wiegman et al. (2022). We predicted MMP above optimum for approximately 31% of the watershed’s agricultural land, with only 2% deemed “excessive.” Wiegman et al. (2022) found that the “excessive” MMP category of >20 mg/kg is near to a PSR threshold based on oxalate extraction, and others have reported relationships between MMP and WEP release to be linear (Jokela et al., 1998; Khiari et al., 2000; Magdoff et al., 1999; Sims et al., 2002).

Possible explanations for lower-than-expected abundance of $PSR > 0.1$ and “excessive” MMP are (1) P losses via surface and subsurface pathways have reduced remaining P in

the soil, (2) past P applications have not been excessive based on existing criteria, and (3) relative abundance of soil P sorption sites reduce the P extracted by the MM solution (Magdoff et al., 1999), which also affects our PSR estimates here. We do not have evidence to fully evaluate each of these possibilities but hypothesize that all three play a role in the MBB. It is also important to note that PSR is best interpreted as a risk factor for dissolved P loss (Dari et al., 2018), and MMP can be used similarly as well as to gauge expected crop yield response (Magdoff et al., 1999). Neither metric inherently captures risk for particulate P loss via erosion, which requires accounting for transport factors in addition to source factors. This is achieved at the field level by tools such as the Vermont P Index (Faulkner, 2021) and can also be estimated in watershed models. The latter is the next step in our research.

5 | CONCLUSIONS

Our analysis suggests that agricultural land in the MBB with highest PSR and MMP values is on flatter ground, with soils having lower permeability, in areas more susceptible to flooding. Our modeling effort is consistent with the findings of others (LCBP, 2022; Meals et al., 2008b; Winchell et al., 2011; Wironen et al., 2018), who have stated that the impacts of legacy soil phosphorus and repeated nutrient balance surplus will continue to impact river and lake water quality for years to come in the region. These findings have direct implications for collective efforts to integrate nutrient management planning with watershed-scale P management activities, such as evaluating potential candidates for wetland restoration (Wiegman et al., 2024) or other BMPs. These results can also directly inform a comprehensive binational modeling project supported by the Lake Champlain Basin Program (Supporting Information S1).

Furthermore, we have pioneered a bottom-up method to predict P balance and soil nutrient status for agricultural land in a $>100,000$ -ha watershed by leveraging field-level management data in our predictions. Our bottom-up approach can be replicated to model nutrient status elsewhere for watersheds having appropriate data sources, with key requirements being access to NMPs that (1) cover a sizable portion of the agricultural land within the watershed, (2) have similar spatial distribution to agricultural land in the watershed, and (3) are largely representative of the agricultural land use types and practices within the watershed. Our study of the MBB clearly met two of those three requirements (NMPs covering 21% of agricultural land area with good spatial distribution) and largely met the third, albeit with some indication of overrepresentation of fields with dairy manure inputs and underrepresentation of fields with fertilizer inputs. The resulting spatial predictions of P balance and soil metrics, with uncertainty analysis, can inform improved models of

P movement as we strive to document the effects of ongoing nutrient management efforts.

AUTHOR CONTRIBUTIONS

Finn A. Bondeson: Data curation; formal analysis; investigation; methodology; visualization; writing—original draft; writing—review and editing. **Joshua W. Faulkner:** Conceptualization; data curation; funding acquisition; methodology; writing—review and editing. **Tiffany L. Chin:** Data curation; formal analysis; investigation; methodology; writing—review and editing. **Andrew W. Schroth:** Conceptualization; funding acquisition; project administration; writing—review and editing. **Michael Winchell:** Conceptualization; data curation; funding acquisition; project administration; writing—review and editing. **Aubert Michaud:** Conceptualization; data curation; methodology; writing—review and editing. **Mohamed Niang:** Data curation; formal analysis; methodology; writing—review and editing. **Eric D. Roy:** Conceptualization; funding acquisition; methodology; supervision; writing—review and editing.

ACKNOWLEDGMENTS

Funding for this project was provided by the United States Environmental Protection Agency under an assistance agreement to NEIWPCC in partnership with the Lake Champlain Basin Program (LC00A00707). This project received funding under award NA22NWS4320003 from NOAA Cooperative Institute Program. The statements, findings, conclusions, and recommendations are those of the authors and do not necessarily reflect the views of NOAA. The funders played no role in the data collection, interpretation, or analysis.

CONFLICT OF INTEREST STATEMENT

The authors declare no conflicts of interest.

ORCID

Andrew W. Schroth  <https://orcid.org/0000-0001-5553-3208>

Eric D. Roy  <https://orcid.org/0000-0001-6315-3061>

REFERENCES

- Arnold, J. G., Srinivasan, R., Muttiah, R. S., & Williams, J. R. (1998). Large area hydrologic modeling and assessment Part I: Model development. *Journal of the American Water Resources Association*, 34(1), 73–89. <https://doi.org/10.1111/j.1752-1688.1998.tb05961.x>
- Chowdhury, R. B., Moore, G. A., Weatherley, A. J., & Arora, M. (2014). A review of recent substance flow analyses of phosphorus to identify priority management areas at different geographical scales. *Resources, Conservation & Recycling*, 83, 213–228. <https://doi.org/10.1016/j.resconrec.2013.10.014>
- Correll, D. L. (1998). The role of phosphorus in the eutrophication of receiving waters: A review. *Journal of Environmental Quality*, 27(2), 261–266. <https://doi.org/10.2134/jeq1998.00472425002700020004x>
- Dari, B., Nair, V. D., Sharpley, A. N., Kleinman, P., Franklin, D., & Harris, W. G. (2018). Consistency of the threshold phosphorus saturation ratio across a wide geographic range of acid soils. *Agrosystems, Geosciences & Environment*, 1(1), 1–8. <https://doi.org/10.2134/age2018.08.0028>
- Engel, B., Smith, M., Fisher, J. B., Olsen, R., & Ahiablame, L. (2013). Phosphorus mass balance of the Illinois River watershed in Arkansas and Oklahoma. *Journal of Water Resource and Protection*, 5(06), 591–603. <https://doi.org/10.4236/jwarp.2013.56060>
- Esri. (2022). *ArcGIS Pro 3.0.3*. Esri.
- Faulkner, J. W. (2021). *Vermont phosphorus index*. University of Vermont Extension. <https://www.uvm.edu/extension/agriculture/vermont-phosphorus-index>
- Ghebremichael, L. T., Veith, T. L., & Watzin, M. C. (2010). Determination of critical source areas for phosphorus loss: Lake Champlain Basin, Vermont. *Transactions of the ASABE*, 53(5), 1595–1604. <https://doi.org/10.13031/2013.34898>
- Hall, P. K., & Essman, E. (2019). *State legal approaches to reducing water quality impacts from the use of agricultural nutrients on farmland*. USDA. https://farmoffice.osu.edu/sites/aglaw/files/site-library/State_Legal_Approaches_to_Agricultural_Nutrients.pdf
- Hartigan, J. A., & Wong, M. A. (1979). Algorithm AS 136: A K-means clustering algorithm. *Journal of the Royal Statistical Society: Series C (Applied Statistics)*, 28(1), 100–108. <https://www.jstor.org/stable/2346830>
- Heathwaite, A. L., Sharpley, A., Bechmann, M., & Rekolainen, S. (2015). Assessing the risk and magnitude of agricultural non-point source phosphorus pollution. *Phosphorus: Agriculture and the Environment*, 46, 981–1020. <https://doi.org/10.2134/agronmonogr46.c30>
- Heathwaite, A. L., Fraser, A. I., Johnes, P. J., Hutchins, M., Lord, E., & Butterfield, D. (2003). The phosphorus indicators tool: A simple model of diffuse P loss from agricultural land to water. *Soil Use and Management*, 19(1), 1–11. <https://doi.org/10.1111/j.1475-2743.2003.tb00273.x>
- Jaworski, N. A., Groffman, P. M., Keller, A. A., & Prager, J. C. (1992). A watershed nitrogen and phosphorus balance: The upper Potomac River basin. *Estuaries*, 15(1), 83–95. <https://doi.org/10.2307/1352713>
- Jokela, W. E., Magdoff, F. R., Bartlett, R., Bosworth, S., Ross, D., & Ruhl, L. (2020). *Nutrient recommendations for field crops in Vermont*. https://www.uvm.edu/sites/default/files/Northwest-Crops-and-Soils-Program/2021%20Events/NMP%20Class/NutrientRec_BR1390.3_Sept2020.pdf
- Jokela, W. E., Magdoff, F. R., & Durieux, R. P. (1998). Improved phosphorus recommendations using modified Morgan phosphorus and aluminum soil tests. *Communications in Soil Science and Plant Analysis*, 29(11–14), 1739–1749. <https://doi.org/10.1080/00103629809370064>
- Khiari, L., Parent, L. E., Pellerin, A., Alimi, A. R. A., Tremblay, C., Simard, R. R., & Fortin, J. (2000). An agri-environmental phosphorus saturation index for acid coarse-textured soils. *Journal of Environmental Quality*, 29(6), 2052–2052. <https://doi.org/10.2134/jeq2000.00472425002900060053x>
- LCBP. (2022). *Opportunities for action: An evolving plan for the future of the Lake Champlain Basin*.
- Maccoux, M. J., Dove, A., Backus, S. M., & Dolan, D. M. (2016). Total and soluble reactive phosphorus loadings to Lake Erie: A detailed accounting by year, basin, country, and tributary. *Journal of*

- Great Lakes Research*, 42(6), 1151–1165. <https://doi.org/10.1016/j.jglr.2016.08.005>
- Magdoff, F. R., Hryshko, C., Jokela, W. E., Durieux, R. P., & Bu, Y. (1999). Comparison of phosphorus soil test extractants for plant availability and environmental assessment. *Soil Science Society of America Journal*, 63(4), 999–1006. <https://doi.org/10.2136/sssaj1999.634999x>
- Meals, D. W., Alan Cassell, E., Hughell, D., Wood, L., Jokela, W. E., & Parsons, R. (2008a). Dynamic spatially explicit mass-balance modeling for targeted watershed phosphorus management. I. Model development. *Agriculture, Ecosystems and Environment*, 127(3–4), 189–200. <https://doi.org/10.1016/j.agee.2008.04.004>
- Meals, D. W., Alan Cassell, E., Hughell, D., Wood, L., Jokela, W. E., & Parsons, R. (2008b). Dynamic spatially explicit mass-balance modeling for targeted watershed phosphorus management. II. Model application. *Agriculture, Ecosystems and Environment*, 127(3–4), 223–233. <https://doi.org/10.1016/j.agee.2008.04.005>
- Michaud, A. R., Beaudin, I., Deslandes, J., Bonn, F., & Madramootoo, C. A. (2007). SWAT-predicted influence of different landscape and cropping system alterations on phosphorus mobility within the Pike River watershed of south-western Québec. *Canadian Journal of Soil Science*, 87(3), 329–344. <https://doi.org/10.4141/S06-046>
- Moore, R. B., McKay, L. D., Rea, A. H., Bondelid, T. R., Price, C. V., Dewald, T. G., & Johnston, C. M. (2019). *User's guide for the national hydrography dataset plus (NHDPlus) high resolution* (Open-file report 80). <http://pubs.er.usgs.gov/publication/ofr20191096>
- NRCS. (2022). Soil survey geographic (SSURGO) database. Soil Survey Staff, Natural Resources Conservation Service, United States Department of Agriculture. <https://sdmdataaccess.sc.egov.usda.gov>
- R Core Team. (2022). R: A language and environment for statistical computing (4.2.2). R Foundation for Statistical Computing. <https://www.r-project.org/>
- Radcliffe, D. E., Freer, J., & Schoumans, O. (2009). Diffuse phosphorus models in the United States and Europe: Their usages, scales, and uncertainties. *Journal of Environmental Quality*, 38(5), 1956–1967. <https://doi.org/10.2134/jeq2008.0060>
- Roy, E. D., White, J. R., & Seibert, M. (2014). Societal phosphorus metabolism in future coastal environments: Insights from recent trends in Louisiana, USA. *Global Environmental Change*, 28, 1–13. <https://doi.org/10.1016/j.gloenvcha.2014.05.009>
- Sabo, R. D., Clark, C. M., Gibbs, D. A., Metson, G. S., Todd, M. J., LeDuc, S. D., Greiner, D., Fry, M. M., Polinsky, R., Yang, Q., Tian, H., & Compton, J. E. (2021). Phosphorus inventory for the conterminous United States (2002–2012). *JGR Biogeosciences*, 126(4), e2020JG005684. <https://doi.org/10.1029/2020JG005684>
- Scavia, D., Bocaniov, S. A., Dagnew, A., Long, C., & Wang, Y. C. (2019). St. Clair-Detroit River system: Phosphorus mass balance and implications for Lake Erie load reduction, monitoring, and climate change. *Journal of Great Lakes Research*, 45(1), 40–49. <https://doi.org/10.1016/j.jglr.2018.11.008>
- Sims, J. T., Maguire, R. O., Leytem, A. B., Gartley, K. L., & Pautler, M. C. (2002). Evaluation of Mehlich 3 as an agri-environmental soil phosphorus test for the mid-atlantic United States of America. *Soil Science Society of America Journal*, 66(6), 2016–2032. <https://doi.org/10.2136/sssaj2002.2016>
- USDA NASS. (2016). *Cropland Data Layer*. USDA NASS. <https://nassgeodata.gmu.edu/CropScape/>
- USDA NASS. (2017). *2017 Census of Agriculture*. <http://www.nass.usda.gov/AgCensus>
- USEPA. (2016). *Phosphorus TMDLs for Vermont segments of Lake Champlain*. USEPA. <http://www.epa.gov/tmdl/total-maximum-daily-load-document-and-appendices-vermont-segments-lake-champlain#file-187891>
- USGS. (2022). *National Hydrography Plus High Resolution (NHDPlus HR)*. United States Geologic Survey. <https://www.usgs.gov/national-hydrography/access-national-hydrography-products>
- VCGI. (2016). Vermont open geodata portal. VCGI. <http://geodata.vermont.gov>
- Wang, Y., Zhang, T., O'Halloran, I., Hu, Q., Tan, C., Speranzini, D., Macdonald, I., & Patterson, G. (2015). Agronomic and environmental soil phosphorus tests for predicting potential phosphorus loss from Ontario soils. *Geoderma*, 241–242, 51–58. <https://doi.org/10.1016/j.geoderma.2014.11.001>
- Wang, Z., Zhang, T., Tan, C., & Qi, Z. (2020). Modeling of phosphorus loss from field to watershed: A review. *Journal of Environmental Quality*, 49(5), 1203–1224. <https://doi.org/10.1002/jeq2.20109>
- Wiegman, A. R. H., Myers, G. H., Augustin, I. C., Kubow, M. L., Fein-Cole, M. J., Perillo, V. L., Ross, D. S., Diehl, R. M., Underwood, K. L., Bowden, W. B., & Roy, E. D. (2022). Potential for soil legacy phosphorus release from restored riparian wetlands within an agricultural landscape. *Biogeochemistry*, 161(2), 137–156. <https://doi.org/10.1007/s10533-022-00972-2>
- Wiegman, A. R. H., Underwood, K. L., Bowden, W. B., Augustin, I. C., Chin, T. L., & Roy, E. D. (2024). Modeling phosphorus retention and release in riparian wetlands restored on historically farmed land. *Journal of Ecological Engineering Design*, 1(1). <https://doi.org/10.21428/f69f093e.a06ba868>
- Winchell, M., Meals, D., Folle, S., Moore, J., Braun, D., Deleo, C., & Budreski, K. (2011). *Identification of critical source areas of phosphorus within the Vermont sector of the Missisquoi Bay Basin* (Technical report no. 63B). Lake Champlain Basin Program.
- Wironen, M. B., Bennett, E. M., & Erickson, J. D. (2018). Phosphorus flows and legacy accumulation in an animal-dominated agricultural region from 1925 to 2012. *Global Environmental Change*, 50, 88–99. <https://doi.org/10.1016/j.gloenvcha.2018.02.017>

SUPPORTING INFORMATION

Additional supporting information can be found online in the Supporting Information section at the end of this article.

How to cite this article: Bondeson, F. A., Faulkner, J. W., Chin, T. L., Schroth, A. W., Winchell, M., Michaud, A., Niang, M., & Roy, E. D. (2024). Watershed-scale spatial prediction of agricultural land phosphorus mass balance and soil phosphorus metrics: A bottom-up approach. *Journal of Environmental Quality*, 53, 1152–1163. <https://doi.org/10.1002/jeq2.20633>